communications sustainability

A Nature Portfolio journal

Article

https://doi.org/10.1038/s44458-026-00085-z

Magnesium silicate binder shows potential as a carbon-neutral route for cement manufacture

Christoph Naber[1] ✉, Juraj Majzlan[2], Nils Moosdorf[3,4], Jürgen Neubauer[5], Daniel Wagner[1] & Frank Bellmann[1,6]

Cement production is responsible for a significant share of global anthropogenic carbon dioxide emissions, largely due to limestone calcination, and is projected to remain a major emitter through mid-century. Identifying materials that could reduce reliance on limestone-based cement therefore remains an important research objective. Here we evaluate a magnesium silicate binder produced from thermally activated serpentinite and examine its technical performance alongside an assessment of raw-material availability. A prospective life-cycle analysis for the European cement sector indicates that replacing or retrofitting existing cement plants to produce this binder could substantially reduce emissions by 2050, depending on future energy systems. Modelled resource estimates suggest that suitable ultramafic rocks are widespread, though data availability varies by region. These findings illustrate the potential of magnesium-silicate-based binders as a prospective lower-carbon pathway for cement production.

The building material concrete basically consists of stone aggregate, water, and the binding phase cement. Among all available cement types, Portland based cement is by far the most widely used. However, its production is associated with high CO_2 emissions. Over 4 billion tons of cement are produced annually, contributing approximately 8% of global CO_2 emissions[1,2]. Of these CO_2 emissions, roughly 40% stem from energy consumption during production while the remaining 60% result from limestone decarbonation[3]. Especially the latter emissions are considered hard to abate, since limestone is the only globally abundant and economically viable source of CaO, which is essential for producing the primary binder phase Ca_3SiO_5 (alite) upon addition of a silica source during high-temperature clinkering.

To reduce greenhouse gas emissions in accordance with the COP21 Paris Agreement[4], the construction sector must adopt effective decarbonisation strategies. Current approaches include lowering the clinker content of cements by adding supplementary materials, improving kiln efficiency, and reducing the cement content in concrete[5]. The remaining hard-to-abate CO_2 emissions from limestone carbonation are targeted for carbon capture, storage, and utilisation (CCSU)[6,7]. However, the widespread adoption of CCSU technology and deployment of CCS facilities has been slow during the last decade since the Paris Agreement[8]. The process is capital intensive and requires the development of entirely new infrastructure for CO_2 capture, transport, and long-term storage. Moreover, the disposal of CO_2 in geological formations is a process unprecedented in nature with uncertain long-term environmental impacts aside from unresolved legal and liability concerns[9].

Our findings open a pathway for carbon-neutral construction by leveraging a nature-inspired and well-studied reaction mechanism to develop a novel and sustainable magnesium silicate binder. This approach avoids the need for CCSU infrastructure, reducing costs and risks. We begin by assessing the thermodynamics and hydration kinetics of this binder system, followed by an enumeration of the global raw material availability. Finally, we discuss the achievable CO_2 emission reduction through 2050 and beyond.

Results

Thermodynamics and kinetics of magnesium silicate hydration

Ultramafic rocks rich in MgO, FeO and Fe_2O_3 are abundant in the Earth's crust and upper mantle. Upon reaction with H_2O-rich fluids[10], they are altered to serpentine and other minerals. Serpentinization is an important geochemical process that is essential for properties of oceanic lithosphere[11,12], has played a pivotal role for the origin of life[13,14], affects water transport into magma during subduction and thus contributes to volcanism and earthquakes[15], impacts geochemical cycling of CO_2 and H_2S[16] and leads

[1]Oliment GmbH, Rötha, Germany. [2]Institute of Geosciences, Friedrich-Schiller University, Jena, Germany. [3]Leibniz Centre for Tropical Marine Research (ZMT), Bremen, Germany. [4]Kiel University, Kiel, Germany. [5]Friedrich-Alexander-Universität Erlangen-Nürnberg, Erlangen, Germany. [6]Bauhaus University Weimar, Weimar, Germany. ✉e-mail: christoph.naber@oliment.de

to enrichment of trace elements relative to primary mantle rocks[17]. Of particular practical relevance, artificially accelerated serpentinization is considered a first step in delivering material for the sequestration of CO_2 which might become indispensable for mitigating climate change[18,19].

There is a certain degree of analogy and certain divergence among the traditional cementitious system CaO-SiO_2 and the emerging system MgO-SiO_2. The two principal calcium silicate phases are Ca_3SiO_5 (alite) and Ca_2SiO_4 (belite). These phases are hydraulic; that is, they react with water and form calcium silicate hydrates (C-S-H), which are mainly responsible for the strength development of cement. Only Ca_2SiO_4 has a structural analogue in the MgO-SiO_2 system. The polymorph $\gamma - Ca_2SiO_2$ is called calcio-olivine and is isostructural with the Mg_2SiO_4 phase forsterite. However, like forsterite, $\gamma - Ca_2SiO_2$ is nonhydraulic. It can be activated by a conversion to a hydraulic x-Ca_2SiO_4 phase (with an actual composition of ~Ca_2SiO_4•0.5H_2O). The x-Ca_2SiO_4 phase is 39.4 ± 6.4 kJ mol^{-1} metastable with respect to $\gamma - Ca_2SiO_2$ and liquid H_2O[20] (all values given here at $T = 298.15$ K and $P = 10^5$ Pa).

The thermodynamic properties of an analogous hydraulic phase x-Mg_2SiO_4 have not yet been experimentally determined. Nevertheless, some parallels can be inferred. The x-phases are typically nanocrystalline. Based on the measured surface energy of forsterite[21], nanocrystalline Mg_2SiO_4 is calculated to be 13.5 kJ mol^{-1} metastable with respect to well crystalline Mg_2SiO_4. Amorphization increases the metastability margin. An extreme case thereof is that of Mg_2SiO_4 glass, which was found to be 71.3 kJ·mol^{-1} metastable with respect to coarse crystalline Mg_2SiO_4[22]. Although the thermodynamic effect of hydration is difficult to quantify precisely, it is reasonable to infer that the Gibbs free energy of the x-Mg_2SiO_4 lies between that of nanocrystalline Mg_2SiO_4 and Mg_2SiO_4 glass, implying a sufficient thermodynamic driving force for hydraulic reactivity (Supplementary Fig. 1).

Both calcium silicate hydrate (C-S-H) and magnesium silicate hydrate (M-S-H) phases are thermodynamically stable relative to their respective anhydrous precursors ($Ca_2SiO_4 + H_2O$ and $Mg_2SiO_4 + H_2O$), assuming that CO_2 is excluded from the system. For the assemblage M-S-H + brucite ($Mg(OH)_2$), the Gibbs free energies for various M-S-H model phases are −14 to −24 kJ mol^{-1} relative to $Mg_2SiO_4 + H_2O$, based on available thermodynamic data[23,24].

The hydration kinetics of Mg_2SiO_4 are considerably slower at ambient temperature and pressure conditions compared to hydration kinetics of Portland cement[25]. In nature, the conversion of olivine to the serpentine-group minerals antigorite, lizardite, and chrysotile ($Mg_3Si_2O_5(OH)_4$) occurs under metamorphic conditions involving elevated temperatures and pressures. The sluggish nature of this reaction has contributed to the prevailing view that magnesium silicates are nonhydraulic, in contrast to their calcium counterparts[26].

However, as we show above, there are several strategies to enhance the reaction kinetics of hydraulic phases, including increasing the reactive surface area and employing thermal or mechanochemical activation. These thermodynamic and kinetic insights form the basis for a binder concept based on a reactive magnesium silicate phase, x-Mg_2SiO_4.

Here we present an environmentally sustainable binder inspired by natural geochemical processes and supported by our thermodynamic and kinetic data. To demonstrate the feasibility of industrial-scale production, we focus on the raw material serpentinite, although other ultramafic rock types are also suitable, as reported in recent patent applications[27,28]. As a proof of concept, the hydraulic activity of this magnesium silicate binder is illustrated in Fig. 1 in comparison with traditional Portland cement, natural forsterite, and serpentinite. Our results show that the binder achieves excellent compressive strength. In their native states, forsterite and serpentinite exhibit no hydraulic activity. However, they become hydraulically active after thermal and mechanical activation, as described below. The comparable performance of the M-S-H binder, combined with its low projected CO_2 emissions, positions it as a promising candidate for the future of sustainable construction materials.

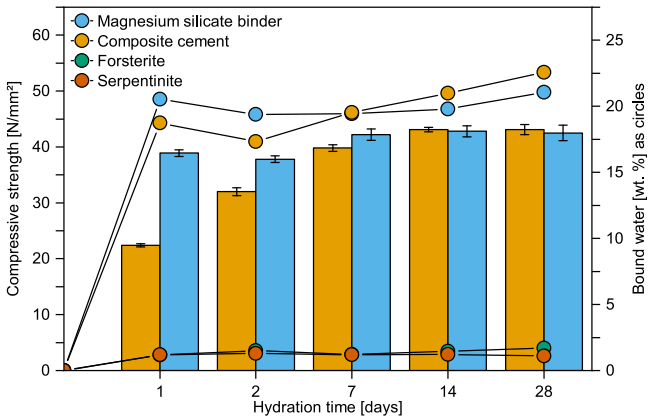

Fig. 1 | Performance of limestone-based cement compared to magnesium silicates as a proof of concept. Compressive strength development of the magnesium silicate binder (MSB), limestone-based composite cement (CEM II B-LL 32.5 R), natural forsterite, and natural serpentinite over 28 days cured at 25 °C as bar graph plotted on the left *y*-axis. Curing of natural forsterite and natural serpentinite does not lead to a measurable compressive strength. Bound water as an indicator of a hydration reaction plotted as circles on the right *y*-axis.

Upscaling of the cementitious binder technology

In the manufacturing process presented here and depicted in Fig. 2, serpentinite rock is mined, comminuted, heat-treated, and ground to a fine powder. Process parameters such as temperature, dwell time, and optimum fineness depend on the raw material and type of equipment used; examples are provided in the Materials section. Most serpentinite rocks contain a certain amount of the serpentine mineral chrysotile which is set free as fibres known as white asbestos during grinding and which pose a certain health risk. Thus, the whole production process from comminution to grinding of the final product needs to be performed as a closed process to prevent the release of asbestos fibres to the environment. Thermal treatment and subsequent grinding is a common method for asbestos fibre disposal[29], the dehydration of the chrysotile fibres leads to reduced stability and grinding reduces the size of the fibres to below the harmful size range defined by the common WHO classification[30]. Performed properly this treatment renders the resulting product of the presented manufacturing process free of any asbestos fibres and safe to use.

The resulting product is a highly reactive powder composed predominantly of X-ray amorphous, partially dehydrated magnesium silicate hydrates, which are presumed to be structurally related to the hydraulic x-Mg_2SiO_4 phase discussed above (Fig. 2b). Upon mixing with water, the reactive powder dissolves gradually, and magnesium silicate hydrates (M-S-H) precipitate via a coupled dissolution-precipitation process (Fig. 2c, d and Eq. 1). M-S-H phases are nanometre-sized, highly disordered analogues of Mg sheet silicates present in serpentinite rocks (Fig. 2h)[31] that exhibit a comparable level of silicate tetrahedra polymerisation (Fig. 2g). The chemical composition of these phases is highly variable, indicated by the operators *x* and *y* in the exemplary Eq. 1 with *x* typically ranging between 1.4 and 3 and *y* typically ranging between 5 and 6.

$$Mg_3Si_2O_7{}^* \sim 0.5H_2O + (\sim 2.5 - x + y)H_2O \rightarrow xMgO{}^*2SiO_2{}^*yH_2O + (3 - x)Mg(OH)_2 \quad (1)$$

The formation of M-S-H phases during hydration is mainly responsible for the increase in compressive strength (Figs. 1 and 2e). Application and handling of the binder is comparable to traditional cement. It is suitable for both ready-mix and precast concrete applications, with a potential advantage for large scale concrete structures like foundations due to the lower heat of hydration (Fig. 2c). Due to the lack of admixtures tailored to the magnesium silicate phases present in the binder[31,32], currently high superplasticizer dosages are needed to achieve an acceptable workability at

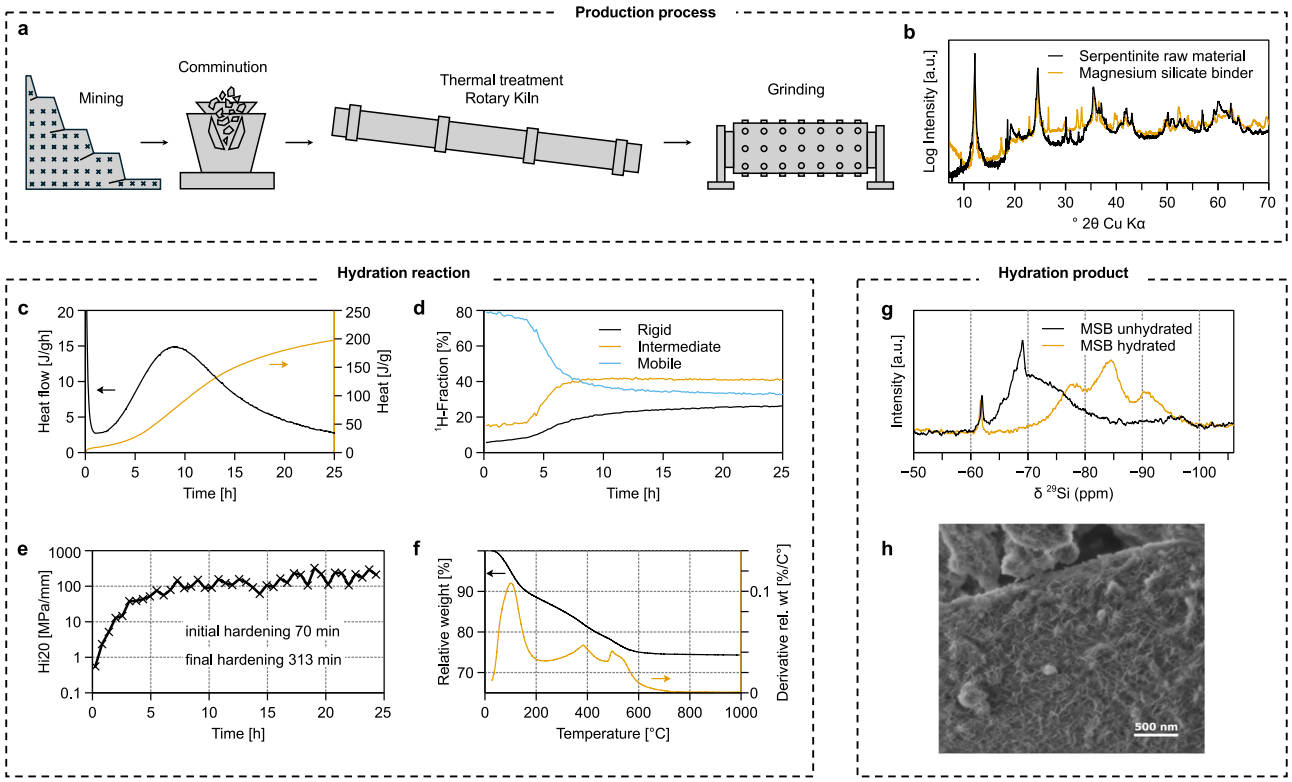

Fig. 2 | Magnesium silicate binder (MSB), from raw material to the final product as tested on an industrial scale. a Production process of MSB. **b** Powder X-ray diffraction patterns of the raw material serpentinite and the magnesium silicate binder resulting from the presented production process. **c** Calorimetric heat flow measurement of hydrating MSB cement paste. **d** ^{1}H-Time domain NMR measurement of iron-free MSB cement over the first 48 h of hydration, display of the hydrogen fractions bound in mixing water, dissolving MSB cement and precipitating hydrate phases. **e** Hardness development of hydrating MSB cement paste. **f** Thermogravimetric analysis of 24 h hydrated MSB cement with the relative weight signal on the left *y*-axis and the derivative thereof on the right *x*-axis. **g** ^{29}Si MAS NMR spectra of unhydrated and 28-day hydrated iron-free MSB cement. **h** SEM image of hardened MSB cement paste (lower right, scale bar 500 nm).

low water-to-binder ratios. Tailor-made additives compatible with the pore solution chemistry and surfaces of the binder phases need to be developed.

The pore solution of concrete structures prepared with magnesium silicate binder has a pH of approximately 10, which is considerably lower than that of conventional concrete made from Portland cement, which has a pH of approximately 13. For concretes reinforced with steel rebar a high pH is usually favoured since it leads to electrochemical passivation of the steel surface hindering corrosion. Recently published literature however indicates that a finer porosity and a low conductivity of the pore solution of M-S-H type binders could compensate for the lower pH with respect to steel corrosion rates[32,33]. Additional precautionary measures may still be needed for certain reinforced concrete applications to prevent steel rebar corrosion. Such measures may include the use of protective coatings for steel rebar, such as hot-dip galvanisation, or alternative reinforcement materials, such as carbon, glass or polymer fibres.

Global raw material availability

Restructuring the cement industry requires demonstrating that an alternative, exploitable resource is globally available. The production of magnesium silicate binder (MSB) depends on ultramafic rocks with variable degree of serpentinization. Rocks with incipient or advanced serpentinization require different treatment processes. Serpentinite rock is currently being used mainly as gravel for road and railroad construction, as a slag former in steel making or as decorative stone, thus there are quarries operational around the world fit for delivering raw material for magnesium silicate binder production. Our analysis of a publicly available geological database[34] demonstrates that source rocks in 28 of the 36 analysed countries suffice to support a shift from traditional cement to MSB lasting for more than 100 years based on the current cement demand (Fig. 3). Moreover, several countries with the potential to export large amounts of ultramafic raw materials can be identified (Supplementary Table 1). However, Fig. 3 also highlights countries where the employed database lacks sufficient data on serpentinite deposits and geological information in general. This is particularly true for parts of South America, most of Africa, the Middle East, and South Asia.

A review of the available literature on serpentinite deposits in Egypt and Nigeria —two major cement-producing countries—is provided in the Supplementary Materials. Due to the increasing demand for concrete, these countries were selected to demonstrate the widespread availability of serpentinite raw material in regions where data availability is limited. In Egypt, serpentinite deposits are associated with Neoproterozoic ophiolites. Although not previously the focus of geological exploration, the available literature lists resources sufficient for more than 100 years of MSB production, based on the assessment procedure described in the Methods section. Literature on Nigerian serpentinite deposits is scarce. Nevertheless, the available literature indicates that serpentinite bodies occur as part of the Proterozoic schist belts in the Precambrian basement complex of Nigeria[35]. The found literature sources amount to ~60 km^2 of serpentinite deposits, translating into 51 years of current annual cement production (Supplementary Table 2 and Fig. 3).

Massive CO_2 reduction potential

The reduction potential for greenhouse gas emissions is twofold for the presented magnesium silicate binder technology. First, since the raw materials are silicate-based and do not contain CO_2, the production process does not release any emissions that are considered hard-to-abate for the traditional cement production. These emissions account for approximately 600 kg of CO_2 per ton of Portland cement clinker produced. Second, the kiln

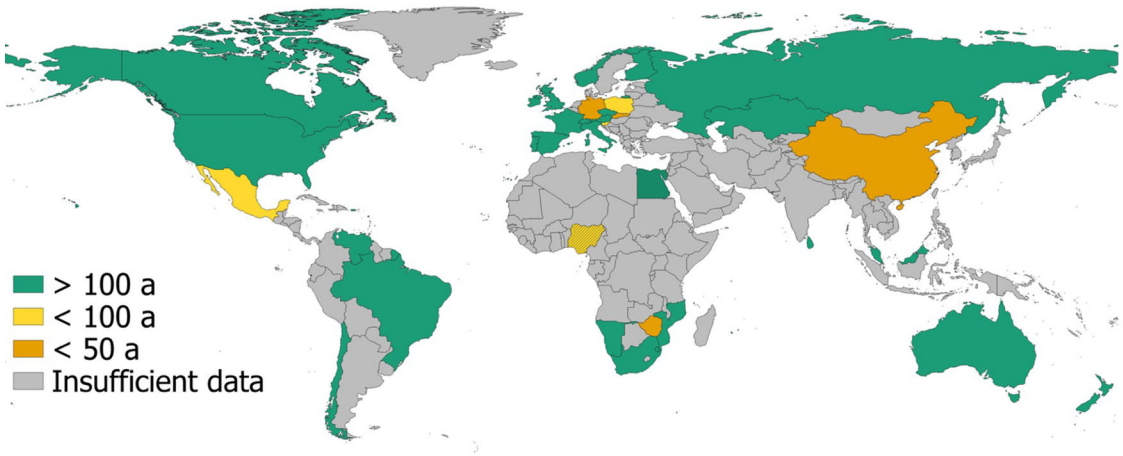

Fig. 3 | Global distribution of serpentinite rocks, suitable for MSB production. Resource ranges were calculated based on the current cement requirements of each country[41] and a publicly available geological database[34]. For countries in grey, there are no data. Egypt and Nigeria are additionally hachured indicating that the resources are calculated based on conducted literature research.

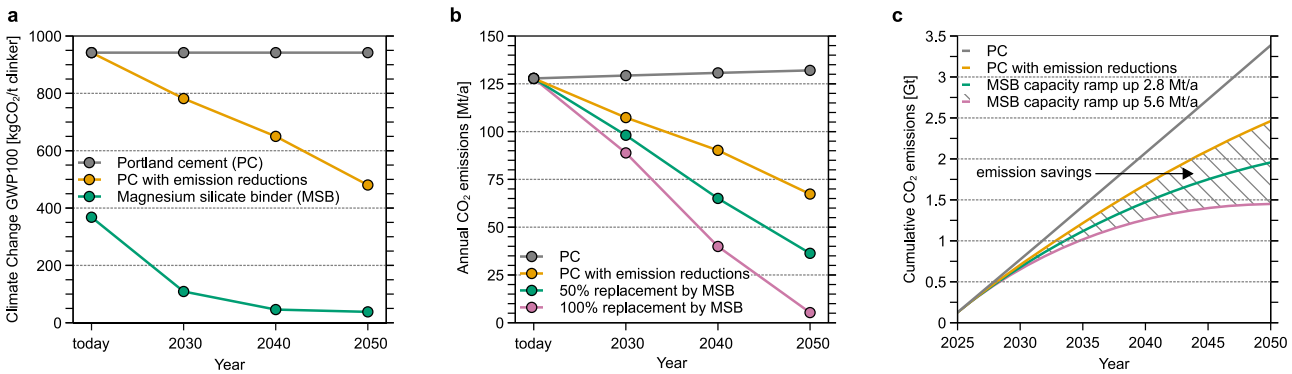

Fig. 4 | Prospective life cycle assessment results for magnesium silicate binder (MSB). a Projected development of the CO_2 emissions of European MSB production up to the year 2050 in kg CO_2/t clinker compared to CO_2 emissions of ordinary Portland cement. **b** projected annual CO_2 emissions from European cement clinker production up to the year 2050 compared to a scenario with 50% replacement of Portland cement by MSB in 2050 and 100% replacement of Portland cement by MSB in 2050. **c** The cumulative CO_2 emissions of the European Portland cement production for the representative pathway for emission reduction measures and two pathways comprising gradual replacement or retrofitting of OPC plants to produce MSB at a ramp-up speed of 2.8 and 5.6 Mt/a production capacity build-up.

temperatures needed for the presented process (up to 800 °C) are substantially lower than those for Portland cement clinker production (1450 °C). These temperatures can be reached by electric heating. If the energy for the produced binder comes from renewable or nuclear sources, the entire process is carbon neutral.

Consequently, the CO_2 emissions associated with magnesium silicate binder production are closely tied to the future development of the energy mix. This development was modelled with a prospective life cycle assessment (pLCA) extending a recently published approach for modelling decarbonisation pathways in the European cement industry[36] with the additional decarbonisation option MSB. Figure 4a shows the projected climate change impact (GWP100) of magnesium silicate binder production in kg CO_2 per ton of cement clinker through 2050 under a scenario of evolving background energy systems[36]. The climate change impact of European Portland cement clinker production up to 2050 is modelled according to a published representative decarbonation pathway of the industry[36] incorporating measures such as clinker factor reduction, the use of alternative fuels and gradual CCS implementation. The modelled CO_2 emissions of 370 kg/t MSB clinker today result from the individual energy mix in the production countries which is still highly dependent on fossil fuels for major cement-producers like Germany and Poland. However, projected changes in the energy mix towards renewable energy sources in the future result in a reduction of the modelled CO_2 emissions.

The modelled annual total CO_2 emissions of the European cement clinker production until 2050 are gradually decreasing from 125 Mt CO_2 today to 70 Mt/a by 2050 for Portland cement clinker production following the representative pathway for emission reductions (Fig. 4b). This reduction in annual CO_2 emissions can be accelerated by the gradual replacement of Portland cement with magnesium silicate binder. A 50% replacement in 2050 corresponds to a linear replacement of 2.8 Mt of production capacity per year starting in 2026, when considering a cement clinker demand of 140 Mt/a in 2050[36]. Likewise, 100% replacement in 2050 corresponds to 5.6 Mt/a production capacity replacement which would mean replacing or retrofitting five to six medium-sized cement plants per year. This way the annual CO_2 emissions will be close to zero in 2050 with only 5 Mt/a, a reduction of 97% compared to the current level.

Discussion

The cumulative CO_2 emissions that can be saved by a 100% replacement of European Portland cement production by MSB with CO_2-neutral electricity in 2050 amount to 2 Gt CO_2 (Fig. 4c), with further savings accruing in subsequent years. Given that Europe accounts for only ~10% of global cement production[3], the CO_2 reduction potential of implementing the presented MSB technology globally is substantially greater and comparable to the combined sum of emissions of global aviation, shipping and rail transport[7].

The raw material serpentinite rock is distributed worldwide and for most regions the available resources vastly exceed the amount needed to replace Portland cement production capacities for more than a century. In areas where geological data are still limited, targeted explorations need to be performed together with local geological surveys and agencies alongside in-depth literature reviews like presented in this work for Egypt and Nigeria to establish suitable material flows for binder production.

Due to its comparable strength development and workability, magnesium silicate binder is capable of replacing Portland cement in a wide variety of concrete applications. Its production process—comprising raw material grinding, thermal activation, and milling—is compatible with existing industrial infrastructure, making it a cost-effective alternative. In contrast, traditional cement production is increasingly burdened by the high cost associated with CO_2 mitigation technologies such as carbon capture, storage, and utilisation (CCSU). Using serpentinite rocks as a source for binder materials also avoids further calcination of limestone, preserving its function as an ideal storage media for CO_2 due to its high stability at conditions of the Earth's surface.

Alongside the production ramp-up and national technical approval processes a deeper understanding of relevant binder and concrete properties such as strength development, durability and miscibility with supplementary cementitious materials needs to be established. The existing literature on M-S-H type binders with different raw materials already indicates a high resistance to carbonation and leaching with a corrosion rate of steel rebar comparable to Portland cement[31–33]. Product development efforts have to be made to replace Portland cement in its broad field of application from mass concrete to construction chemistry formulations.

This study demonstrates that the technological basis for achieving carbon-neutral concrete production by 2050 is technically feasible. At the same time the chosen timeline is quite ambitious given the multitude of challenges described above. Further development and implementation of this approach could contribute substantially to reducing emissions in the construction sector and support long-term climate mitigation goals.

Methods

Materials

Magnesium silicate binder was prepared using serpentinite-type rocks as raw materials from an active quarry in Poland. The stone was crushed to a mean particle size of 6.9 µm, homogenised and heated in a pilot plant scale rotary kiln. Heating was performed at 775 °C. During heating the serpentinite minerals present are partially dehydrated, leading to X-ray-amorphous hydraulically reactive magnesium silicate hydrates. The resulting powder was ground to a fineness of 16,000 cm^2/g.

Compressive strength

Mortar prisms (40 × 40 × 160 mm) were prepared by mixing 450 g of magnesium silicate binder, the reference CEM II/ BB-LL 32.5 R, the raw material serpentinite or natural forsterite with 1350 g of standard sand according to Din EN 196-1. Due to the lower water demand, a water-to-binder ratio of 0.33 and 3 wt% of polycarboxylate ether (PCE) superplasticizer relative to the binder weight were used for the magnesium silicate binder. A water-to-binder ratio of 0.5 was used for the CEM II/ BB-LL 32.5 R, raw material serpentinite and natural forsterite samples. The prisms were demoulded after 1 day and cured underwater at 25 °C. Compressive strength was tested after 1, 2, 7 and 28 days of curing.

Bound water

The water binding capacities of the magnesium silicate binder, CEM II/BB-LL 32.5R, raw material serpentinite and forsterite were tested by measuring the loss on ignition (LOI) at 1000 °C. The samples were prepared by mixing the various binder materials with a water-to-binder ratio of 0.33 and 3% polycarboxylate ether (PCE) superplasticizer relative to the binder weight. After mixing, the samples were placed into PE boxes and stored for specific periods (1, 7, 14 and 28 days). Prior to determining the loss on ignition (LOI), the hydration process was stopped by crushing the samples in a mortar, followed by drying them in an oven at 60 °C for 24 h. For all samples, the bound water content was adjusted to account for the natural water and carbonate content of the materials, by measuring and subtracting the LOI of the unhydrated samples. This corrects, e.g. for the calcium carbonate present in the CEM II/ BB-LL 32.5 R that is calcined during the LOI measurement (11.11 wt%) and the crystalline water bound in the serpentinite (13.34 wt%) and the magnesium silicate binder (1.59 wt%).

X-ray diffraction

X-ray diffraction measurements were performed on a D8 Advance Eco diffractometer (BRUKER-AXS, Germany) with a Cu Kα source and an energy-dispersive detector. Diffractograms were recorded over an angular range of 3–120°2θ with a step size of 0.01°2θ and 0.1 s counting time per step.

Hardness development

The hardness development of the hydrating magnesium silicate binder paste was measured with a Gillmore needle apparatus according to the IMETER method (MSB Breitwieser, Germany). The experiments were performed at a water-to-binder ratio of 0.33 at 23 °C and 85% r. h. During the measurement, the hydrating paste was periodically lifted against a cylindrical needle indenter (weight: 213.3 g, needle diameter: 6.92 mm, maximum speed 3.8 mm/s) connected to an analytical balance. The sample hardness H_{i20} was calculated according to Eq. 2, where F_{max} is the force of the needle exerted on the sample, d is the penetration depth, and A is the area of the needle tip.

$$H_{i20} = F_{max}/(d_{F\,max} * A) \quad (2)$$

Heat flow calorimetry

The heat release during the hydration reaction of the magnesium silicate binder was measured with a TAM Air heat flow calorimeter (TA Instruments, USA) at an elevated water-to-binder ratio of 0.8 and a temperature of 25 °C.

Thermogravimetric and differential thermal analysis

Thermogravimetry (TGA) and differential scanning calorimetry (DSC) of the hydrated magnesium silicate binder were measured at an SDT Q 600 simultaneous DSC/TGA (TA Instruments, USA) in a temperature range of 25–1000 °C at a heating rate of 10 °C/min under a constant N_2 purge gas flow of 100 ml/min.

^{29}Si MAS NMR

The analysis by NMR requires the production of synthetic samples without iron as a foreign element prior to the experiments. The samples were analysed by ^{29}Si solid-state magic angle spinning (MAS) nuclear magnetic resonance (NMR) spectroscopy using an Oxford wide-bore magnet (11.7T), a Bruker Avance III 500 console and a probe head from NMR service Erfurt for 7 mm (O.D.) zirconia rotors. The single-pulse experiments used a MAS spinning rate of 4 kHz, a $\pi/2$ pulse length of 8 µs, 256 scans and a recycle delay time of 180 s. All chemical shift data is reported relative to external tetramethylsilane (TMS).

^{1}H time domain NMR

^{1}H-time-domain-NMR measurements were performed on a minispec mq20 spectrometer (Bruker, Germany) operating at 19.95 MHz. Magensium silicate binder was mixed with water at a water-to-binder ratio of 0.75, transferred into glass vials and placed in the temperature controlled probe head at 23 °C. T2 spin-spin relaxation measurements were performed using solid-echo[37] (also called quadrature-echo) and CPMG (Carr-Purcell-Meiboom-Gill)[38,39] pulse sequences. The T2 relaxation results were evaluated using Gaussian and exponential decay functions for the solid-echo measurements [13] and multiexponential fitting (sum of four exponential decay functions, Levenberg-Marquard fitting algorithm) for the CPMG measurements. Three ^{1}H reservoirs could be distinguished according to their

relaxation times termed 'mobile', 'intermediate' and 'rigid' in Fig. 2 that can be ascribed to hydrogen in mixing water, hydrogen bound in the amorphous binder starting material and precipitating M-S-H phase and hydrogen rigidly bound potentially to precipitating $Mg(OH)_2$.

Electron microscopy

Scanning Electron Microscopy (SEM) images of 72 h hydrated magnesium silicate binder samples with were taken with a Nova NanoSEM (FEI, Netherlands) with no conductive coating at low current settings (2 kV, 16 pA).

Raw material availability analysis

To assess the worldwide ultramafic rock resources, we analysed a publicly available geological database[34] comprising the lithology, location and surface area covered of serpentinite deposits. These deposits were identified in the database by incorporating all data with the term 'serpentine' or 'serpentinite' in the rock description. To account for potential overestimation of the area, we assumed a general rock thickness of 10 metres, which is necessary due to the complex tectonics of ultramafic deposits. The methodology used to calculate resource potential follows a similar approach to other large-scale resource reviews[40]. It involves a straightforward multiplication of the estimated area and thickness. The resulting quantity was then adjusted based on the known characteristics of the rock types involved, as determined through analysis of published literature. To present the potential for MSB production in individual countries, the cement forecast for each country[41] is replaced by 100% MSB production. Based on these calculations, an estimate of the respective range of MSB production can be made (Supplementary Table 1).

For some countries, the GLiM database overlooks ultrabasic rock occurrences, which we showed for Egypt and Nigeria (Supplementary Table 2); neither of these countries had ultrabasic rocks mapped in the GLiM, but individual literature analysis showed their presence, which was added to our raw material availability analysis. However, the examples of these two countries also show that the rock availability shown here is only a very coarse approximation and more detailed studies of the availability of potential source rocks need to be performed at the regional scale as part of a business development.

Prospective life cycle assessment (pLCA)

The prospective life cycle assessment (pLCA) in this study was performed following recently published methods[36]. The goal of the assessment was to evaluate the potential climate impact of replacing conventional Portland cement with magnesium silicate binder (MSB) and to provide insights for industry, research, and policy on decarbonisation strategies. The scope of the study was defined by a functional unit of one metric ton of clinker, considering prospective scenarios up to 2050 under evolving energy mixes. Equivalent to Portland cement production, the term clinker refers to a magnesium silicate binder without the addition of supplementary cementitious materials. Climate change impact was assessed using the GWP100 metric, and background life-cycle inventories were sourced from the database ecoinvent 3.6[42]. Prospective databases were generated using *premise*[43], integrating the scenario 'PKbudget1300' from the Integrated Assessment Model (IAM) REMIND[44]. In addition, the impact on human health, water depletion and fossil fuel use was assessed and is presented in Supplementary Table 4. The system boundaries include raw material extraction, thermal activation, and milling of the binder, as well as associated energy consumption. Downstream processes such as concrete production, use phase, and end-of-life scenarios were excluded. The input data for the production process are presented in Supplementary Table 3. The raw material serpentinite was modelled using the dataset 'market for lime' as a proxy.

Data availability

The data supporting the findings of this study are available in the main text, the supplementary information file and in a publicly available repository[45].

Received: 3 October 2025; Accepted: 28 April 2026;
Published online: 13 May 2026

References

1. Olivier, J., Janssens-Maenhout, G., Muntean, M. & Peters, J. Trends in global CO_2-emissions. 2016 Report. https://www.pbl.nl/sites/default/files/downloads/pbl-2016-trends-in-global-co2-emisions-2016-report-2315_4.pdf (2016).
2. Lehne, J. & Preston, F. Making concrete change: innovation in low-carbon cement and concrete | Chatham House – International Affairs Think Tank. https://www.chathamhouse.org/2018/06/making-concrete-change-innovation-low-carbon-cement-and-concrete (2018).
3. Scrivener, K., John, V. & Gartner, E. Eco-efficient cements: potential economically viable solutions for a low-CO_2 cement-based materials industry. *Cem. Concr. Res*. **114**, 2–26 (2018).
4. UNFCC. *Report of the Conference of the Parties on Its Twenty-First Session, Held in Paris from 30 November to 11 December 2015. (United Nations Framework Convention on Climate Change (UNFCC))*. (2016).
5. Habert, G. et al. Environmental impacts and decarbonization strategies in the cement and concrete industries. *Nat. Rev. Earth Environ.* **1**, 559–573 (2020).
6. *IEA (2020), Energy Technology Perspectives 2020, IEA, Paris* https://www.Iea.Org/Reports/Energy-Technology-Perspectives-2020, *Licence: CC BY 4.0*. (2020).
7. *Industry.*In *IPCC, 2022: Climate Change 2022: Mitigation of Climate Change. Contribution of Working Group III to the Sixth Assessment Report of the Intergovernmental Panel on Climate Change* (eds Shukla, P.R. et al.) https://doi.org/10.1017/9781009157926.013 (Cambridge University Press, 2022).
8. Martin-Roberts, E. et al. Carbon capture and storage at the end of a lost decade. *One Earth* **4**, 1569–1584 (2021).
9. Havercroft, I., Macrory, R. & Stewart, R. Carbon Capture and Storage - Emerging Legal and Regulatory Issues. https://www.bloomsbury.com/uk/carbon-capture-and-storage-9781509909582/.
10. Seyfried, W. E., Foustoukos, D. I. & Fu, Q. Redox evolution and mass transfer during serpentinization: an experimental and theoretical study at 200 °C, 500 bar with implications for ultramafic-hosted hydrothermal systems at Mid-Ocean Ridges. *Geochim. Cosmochim. Acta* **71**, 3872–3886 (2007).
11. Kelley, D. S. et al. An off-axis hydrothermal vent field near the Mid-Atlantic Ridge at 30 degrees N. *Nature* **412**, 145–149 (2001).
12. Früh-Green, G. L. et al. 30,000 years of hydrothermal activity at the lost city vent field. *Science* **301**, 495–498 (2003).
13. McCollom, T. M. Methanogenesis as a potential source of chemical energy for primary biomass production by autotrophic organisms in hydrothermal systems on Europa. *J. Geophys. Res.* **104**, 30729–30742 (1999).
14. Russell, M. J., Hall, A. J. & Martin, W. Serpentinization as a source of energy at the origin of life. *Geobiology* **8**, 355–371 (2010).
15. Rüpke, L. H., Morgan, J. P., Hort, M. & Connolly, J. A. D. Serpentine and the subduction zone water cycle. *Earth Planet. Sci. Lett.* **223**, 17–34 (2004).
16. Alt, J. C. et al. The role of serpentinites in cycling of carbon and sulfur: Seafloor serpentinization and subduction metamorphism. *Lithos* **178**, 40–54 (2013).
17. Deschamps, F., Guillot, S., Godard, M., Andreani, M. & Hattori, K. Serpentinites act as sponges for fluid-mobile elements in abyssal and subduction zone environments. *Terra Nova* **23**, 171–178 (2011).
18. Lackner, K. S. A guide to CO_2 sequestration. *Science* **300**, 1677–1678 (2003).
19. Matter, J. M. et al. Rapid carbon mineralization for permanent disposal of anthropogenic carbon dioxide emissions. *Science* **352**, 1312–1314 (2016).
20. Grevel, K.-D. et al. Thermodynamic data of belite polymorphs. *Cem. Concr. Res.* **152**, 106621 (2022).

21. Chen, S. & Navrotsky, A. Calorimetric study of the surface energy of forsterite. *Am. Mineral.* **95**, 112–117 (2010).
22. Majzlan, J., Tangeman, J. A. & Dachs, E. Heat capacity, entropy, configurational entropy, and viscosity of magnesium silicate glasses and liquids. *Phys. Chem. Miner*. **48**, 28 (2021).
23. Robie, R. A. & Hemingway, B. S. *Thermodynamic Properties of Minerals and Related Substances at 298.15 K and 1 Bar (10^5 Pascals) Pressure and at Higher Temperatures*. *Bulletin* https://pubs.usgs.gov/publication/b2131 https://doi.org/10.3133/b2131 (1995).
24. Bernard, E., Lothenbach, B., Rentsch, D., Pochard, I. & Dauzères, A. Formation of magnesium silicate hydrates (M-S-H). *Phys. Chem. Earth Parts ABC* **99**, 142–157 (2017).
25. Oelkers, E. H., Declercq, J., Saldi, G. D., Gislason, S. R. & Schott, J. Olivine dissolution rates: a critical review. *Chem. Geol.* **500**, 1–19 (2018).
26. Walling, S. A. & Provis, J. L. Magnesia-based cements: a journey of 150 years, and cements for the future? *Chem. Rev.* **116**, 4170–4204 (2016).
27. Bellmann, F. Sequestration of CO_2 - WO2023/134849A1 (2023).
28. Bellmann, F. Method for producing a hydrated cement - WO2025/012209A1 (2025).
29. Spasiano, D. & Pirozzi, F. Treatments of asbestos containing wastes. *J. Environ. Manage.* **204**, 82–91 (2017).
30. International Labour Organization. C162 Asbestos Convention, 1986 (no 162): convention concerning safety in the use of asbestos https://normlex.ilo.org/dyn/nrmlx_en/f?p=NORMLEXPUB:12100:0::NO:12100:P12100_INSTRUMENT_ID:312307:NO (entry into force 16 June 1989).
31. Sreenivasan, H. et al. A critical review of magnesium silicate hydrate (M-S-H) phases for binder applications. *Cem. Concr. Res.* **178**, 107462 (2024).
32. Lothenbach, B. et al. Critical review of the properties of MgO - magnesium carbonate cements. *Cem. Concr. Res.* **200**, 108092 (2026).
33. Meng, D., Yang, E.-H. & Qian, S. Corrosion behavior of steel reinforcement in magnesium silicate hydrate (M-S-H) concrete. *Cem. Concr. Res.* **193**, 107858 (2025).
34. Hartmann, J. & Moosdorf, N. The new global lithological map database GLiM: a representation of rock properties at the Earth surface. *Geochem. Geophys. Geosystems* **13**, Q12004 https://doi.org/10.1029/2012GC004370 (2012).
35. Mücke, A. Chemical composition of chromite and intergrown chlorite in metamorphosed ultramafic rocks (serpentinite and talc schist) of the Egbe-Isanlu schist belt, southwest Nigeria: genetic implications. *J. Min. Geol.* **47**, 115–134 (2011).
36. Cavalett, O., Watanabe, M. D. B., Voldsund, M., Roussanaly, S. & Cherubini, F. Paving the way for sustainable decarbonization of the European cement industry. *Nat. Sustain.* **7**, 568–580 (2024).
37. Powles, J. G. & Strange, J. H. Zero time resolution nuclear magnetic resonance transient in solids. *Proc. Phys. Soc.* **82**, 6 (1963).
38. Carr, H. Y. & Purcell, E. M. Effects of diffusion on free precession in nuclear magnetic resonance experiments. *Phys. Rev.* **94**, 630–638 (1954).
39. Meiboom, S. & Gill, D. Modified spin-echo method for measuring nuclear relaxation times. *Rev. Sci. Instrum* **29**, 688–691 (1958).
40. Bide, T. P., Styles, M. T. & Naden, J. An assessment of global resources of rocks as suitable raw materials for carbon capture and storage by mineralisation. *Appl. Earth Sci.* **123**, 179–195 (2014).
41. *CemNet (2024) - The Global Cement Report 15th Edition*.
42. Wernet, G. et al. The ecoinvent database version 3 (part I): overview and methodology. *Int. J. Life Cycle Assess.* **21**, 1218–1230 (2016).
43. Sacchi, R. et al. PRospective EnvironMental Impact asSEment (*premise*): a streamlined approach to producing databases for prospective life cycle assessment using integrated assessment models. *Renew. Sustain. Energy Rev.* **160**, 112311 (2022).
44. Baumstark, L. et al. REMIND2.1: transformation and innovation dynamics of the energy-economic system within climate and sustainability limits. *Geosci. Model Dev.* **14**, 6571–6603 (2021).
45. Naber, C. et al. Magnesium silicate binder shows potential as a carbon-neutral route for cement manufacture. https://doi.org/10.5281/zenodo.19448965 (2026).

Acknowledgements

The authors thank Otavio Cavalett for contributing to the prospective life cycle assessment calculations and Florian Rafalsky for performing the TD-NMR and IMETER measurements. F.B., D.W. and C.N. thank SPRIND GmbH for supporting the development of the magnesium silicate cement described herein. This work was partly funded by the Deutsche Forschungsgemeinschaft (DFG, German Research Foundation) – 519379450.

Author contributions

F.B. originated the idea. F.B. and J.N. conceived the paper. N.M., D.W. and C.N. performed the resource assessment. J.M. contributed the thermodynamics part. D.W. performed the analytical measurements. C.N. wrote the manuscript's first version, gathered and analysed the data, and all authors reviewed the manuscript.

Competing interests

F.B., D.W. and C.N. are affiliated with a company developing related technologies; all data and analysis are presented objectively.

Additional information

Supplementary information The online version contains supplementary material available at https://doi.org/10.1038/s44458-026-00085-z.

Correspondence and requests for materials should be addressed to Christoph Naber.

Peer review information Communications Sustainability thanks the anonymous reviewer(s) for their contribution to the peer review of this work. Primary Handling Editors: Sean Low and Nandita Basu. A peer review file is available.